Technical report; TR-237

KNMI

Tracing water masses in the Atlantic

Yann Friocourt and Sybren Drijfhout

Koninklijk Nederlands Meteorologisch Instituut

De Bilt, 2001

Technical Report = Technisch Rapport; TR-237

De Bilt, 2001

PO Box 201, 3730 AE De Bilt
The Netherlands
Wilhelminalaan 10
http://www.knmi.nl
Telephone +31 30 22 06 911
Telefax +31 30 22 10 407

Author: Friocourt, Y
Drijfhout, S.S.

UDC: 551.526.63
551.465.5
(261)

ISSN: 0169-1708

ISBN: 90-369-2199-6

Université Paris-Sud - Orsay (France)
Magistère de Physique

Second-year Internship
(7 April - 28 July 2001)

Tracing Water Masses in the Atlantic

Yann FRIOCOURT

Supervisor: **Dr Sybren Drijfhout**

Koninklijk Nederlands Meteorologisch Instituut

Wilhelminalaan 10
PO Box 201
3730 AE De Bilt
The Netherlands

Contents

List of Tables

List of Figures

Acknowledgments

I would like to express my sincere gratitude to Dr Sybren Drijfhout who welcomed me at the KNMI and supervised me during these four months. I am also very grateful to Dr Pedro De Vries and Dr Wilco Hazeleger for valuable advice and fruitful discussions. I would also like to thank John Donners who lent me a bike. I finally thank all the members of the Oceanografisch Onderzoek group for their friendliness.

1 Introduction

The central topic of the Oceanographic Research Division at the Koninklijk Nederlands Meteorologisch Instituut is the study of the role of the oceans and the air/sea interaction in the climate system. The ultimate goal is understanding the natural climate variability, the prediction of climate and the assessment of anthropogenic climate changes. The division focuses on natural climate variability and its causes as it is vital for the prediction of climate and the identification of anthropogenic changes. The research in the division can be divided in three main themes:

- study of the interannual variability (understanding and prediction of "El Niño" events) and the variability of the wind-driven and thermohaline circulations;
- parametrisation and experimental determination of air/sea fluxes;
- prediction of ocean waves.

All these topics are aimed at developing of cutting edge reliable coupled models that can be used for climate forecasts on seasonal to centenial timescales.
The work done during my internship was part of the international project TRACMASS. The aim of this European-funded project is to trace the pathways of the Conveyor Belt in ocean models, using Lagrangian techniques. The TRACMASS program mainly focuses on the water mass circulations in the North Atlantic Ocean and the Mediterranean Sea, and the connections with the other basins of the global ocean.

2 The Conveyor Belt

The global ocean is a major component of the climate system because of its role in the transport of heat and freshwater throughout the world:

- the oceans carry about the same amount of heat from the equator to the poles as the atmosphere;
- the sea water has a much larger heat capacity than the atmosphere, and thus acts as a long-term memory for the world climate system;
- there is a permanent exchange of heat and freshwater between the surface layers of the ocean and the atmosphere.

The mass of water depends on temperature, salinity and pressure. The changes in the properties of a water mass mainly occur in the surface layers through the exchanges with the atmosphere. As a consequence, the properties of deeper waters remain more or less constant in time, or at least vary very slowly. As gravity stratifies the ocean, denser waters tend to sink under lighter ones. Density differences also create pressure gradients which are able to put water masses into movement. The circulation of currents resulting from the differences in densities throughout the world ocean is called the *thermohaline circulation.*

2.1 The North Atlantic Deep Water

The water in the polar and subpolar regions is relatively dense ($\sigma_0 > 27.5$)[1] in spite of the excess of precipitation, because of its cold temperature ($< 4°C$). For instance, dense waters that sink to the bottom are produced in the Greenland and the Norwegian basins. These waters fill the basins up to the level of the Scotland-Iceland-Greenland Ridge, and overflow southward into the North Atlantic Ocean following the topography. Overflows are generally hydrodynamically unstable. As a consequence a turbulent entrainment takes place: the outflowing waters and the surrounding ones mix, thus changing properties. The importance of the mixing is linked with the size of the bottom slope and the initial density difference between the outflow and the oceanic waters. The turbulent entrainment approximately doubles the volume of the flow [4, 11]. North Atlantic Deep Water (NADW) is defined as the southward flow resulting from the confluence of the Scotland-Iceland-Greenland Ridge overflows with Labrador Sea Water (LSW) and Antarctic Bottom Water (AABW). According to estimates NADW transports about 13 Sverdrup (1 Sv $= 10^6 m^3 s^{-1}$) southwards at Cape Farewell [4]. As NADW flows southward in the deep ocean, there must be a northward flow to close the cycle. By comparisons of salinity and concentration in tracers, NADW has been proved to upwell in all the world's basins [7], thus evidencing a global-scale circulation called *the Conveyor Belt* [3].

[1] In oceanography the non-dimensional quantity σ is defined as $\sigma = 1000(\frac{\rho}{\rho_m} - 1)$ where ρ is the density of seawater and ρ_m the density of pure water.

NADW flows southward down to $45°S$, where most of it joins the Antarctic Circumpolar Current (ACC). In the ACC, NADW mixes with Antarctic waters to become Circumpolar Deep Water (CDW). Most of CDW is thought to circle many times around Antarctica, gradually upwelling up to the surface where the water is ventilated. Surface waters are then brought northwards into the different basins by the Ekman transport [5]. They recirculate through all ocean basins. Finally, water flows back from the Pacific into the Atlantic in the upper layers, either through the Indonesian islands (the so-called Indonesian Throughflow) or to the south of Australia, and then around the tip of Africa through the Agulhas leakage, or between South America and Antarctica (the so-called Drake Passage). It then flows northwards in the Atlantic up to the Nordic seas where it downwells again, thus completing the cycle.

2.2 The Mediterranean inflow and outflow

Because of the strong evaporation and the deficit of precipitation over the Mediterranean basin, the water is highly salty (salinity $S = 38.4\,psu$) and thus very dense ($\sigma_0 = 28.95$). It is even denser than the North Atlantic bottom water ($\sigma_0 = 27.9$) and as a result much heavier than the surface waters just outside the Mediterranean. This strong horizontal pressure gradient draws relatively fresh and warm water from the Atlantic into the Mediterranean through the narrow and shallow Gibraltar Strait, whereas the much denser Mediterranean deep water forms an outflowing layer. The dense Mediterranean waters cascade down the continental shelf and slope into the Gulf of Cadiz in the North Atlantic ocean [11].
The Mediterranean outflow does not sink to the bottom of the North Atlantic because it entrains a significant volume of lighter, cooler and fresher North Atlantic Central Water (NACW) as it flows in the Gulf of Cadiz. This entrainement reduces the temperature, salinity and density of the outflow.

2.3 The eddy-induced circulation

The phenomena which have timescales shorter than the seasonal cycle are generically called *eddies*.
Most important are the mesoscale eddies. Many ocean currents are hydrodynamically unstable. Small perturbations grow into large meanders which subsequently break and are cut-off from the parent stream. The cut-off meanders develop into nearly circular symetric cold and warm core anomalies with a diameter of $O(100\ km)$. These mesoscale eddies on the average transport momentum from the top to the bottom of the ocean. The associated eddy-stresses drive the circulations beneath the wind-driven mixed layer. They enhance recirculations north and south of the eastward and westward flowing jets [8].
They also mix tracers and potential vorticity within these gyres to near homogeneous values which enables strong circulations, as circulation is at first order constrained to follow contours of potential vorticity [9, 10].

Eddies counteract wind-driven overturning cells which, without the eddies, would imply strong water mass transformation as the flow apparently crosses isopycnals[2]. As a consequence eddies reduce the net water mass transformation below the mixed layer where the mixing is believed to be weak, by reducing divergencies in the mass flux field on isopycnal surfaces.
Another effect of eddies on watermass transformations occurs at the surface. Winter cooling transforms water mass properties at the surface and deepens the mixed layer. Thus more water is transformed. In spring the mixed layer recedes and transformed water "subducts" in the thermocline. Eddies make the mass flux at the base of the mixed layer stronger and enhance subduction of mixed layer water. They increase water mass transformation in the mixed layer.

[2]An isopycnal is a surface of constant density.

3 Methodology

3.1 The OCCAM global ocean model

The OCCAM model has been developed by the Southampton Oceanographic Center in collaboration with the Universities of East Anglia and Edinburgh.
OCCAM is a primitive equation[3] numerical model of the global ocean. It is based on the Bryan-Cox-Semtner ocean general circulation model, but includes a free surface and improved advection schemes.
The model prognostic variables are potential temperature[4], salinity, horizontal velocity, and sea surface elevation. The pressure, potential density and vertical velocity are diagnosed from these variables.
To overcome the singularity at the North Pole due to the convergence of meridians, OCCAM is split into two different models. Model 1 uses a regular latitude-longitude grid which covers the Pacific, Indian and South Atlantic Oceans. Model 2 uses a rotated latitude-longitude grid and covers the North Atlantic and Arctic Oceans. Both models have a resolution of 0.25° both in latitude and longitude. This corresponds to a resolution of about 25 km at the equator. The two models are connected through the Bering Strait by a simple channel model.
The OCCAM model has 36 levels in the vertical, which thickness varies from 20 m at the surface to 255 m at a depth of 5500 m.
The model uses normal Laplacian diffusion and momentum terms to represent horizontal mixing. The value of the horizontal diffusion coefficient for diffusion of tracers is 100 m^2s^{-1}. The horizontal viscosity for the velocity field is 200 m^2s^{-1}. These values are similar to those observed in the ocean at scales of 20 to 30 km. Laplacian mixing in the vertical with a coefficient of 1 cm^2s^{-1} is applied to the velocity field.
The model depths were calculated from the US Navy DBDB5 dataset. The main sills and channels were checked against results from surveys. The potential temperature and salinity were initialised from the Levitus 82 global annual average dataset. Surface values are relaxed to the Levitus 94 observed monthly means. The velocity field is forced with wind stresses from the ECMWF.
The results from the last three years of a fifteen-year run where used in this study.

3.2 The Lagrangian method

Because models use grids, the variables are known at fixed points in the ocean, as functions of time. Consequently, models describe the oceanic circulation in Eulerian terms. New techniques have now been developed to analyse data in Lagrangian terms by following individual trajectories [1, 2, 5, 6].
It is possible to use time-dependent calculations of trajectories but they are much more time consuming [6]. The following algorithm calculates exact solutions for stationary velocity fields [1].

[3] Bryan's primitive equations are quickly introduced in the appendix p. 18.

[4] The potential temperature is the effective temperature of a parcel of water after removing the heat of the parcel associated solely with compression, that is relative to a pressure of one atmosphere. It remains constant under adiabatic changes in pressure.

The three components of the velocity are known over the six faces of each grid cell. The nondivergence of the velocity field ensures continuous trajectories within this cell. The eastward transport for each grid cell is the eastward velocity multiplied by the area of the eastern face of the cell. This transport can be described by a large number of particles, each one being associated with a part of the flow. The area of each grid cell is divided into small regions, each of them being associated with a particle, so that each particle carries about the same fixed transport, number which is smaller than a prescribed value T_0. This criterion enables particles to be grouped in regions where the transport is the highest [1]. These individual trajectories are computed assuming the conservation of the infinitesimal mass for each particle along its trajectory. A current can be entirely described by the transport of its particles. Thus the transport of a given water mass can be calculated using its particles and their associated infinitesimal transport. The number of particles used has to be large enough to limit the divergence of the routes of the neighbouring particles [5]. The volume transport through the eastern wall of the i, j, k grid cell is given by

$$U_{i,j,k} = \frac{1}{4}(u_{i,j,k} + u_{i,j-1,k} + u_{i,j-1,k-1} + u_{i,j,k-1})\Delta y \Delta z_k \tag{1}$$

in which i, j, k denote the discretised longitude, latitude and depth respectively, u is the zonal velocity and $\Delta y_j \Delta z_k$ is the area of the eastern face of the grid cell. The meridional transport is defined similarly and the vertical one results from the non-divergency of the velocities.
The volume transport inside a grid box is obtained by linear interpolation between the opposite walls [1]. The zonal transport at a distance $r = x/\Delta x_j$ is:

$$F(r) = F_{i-1} + (r - r_{i-1})(F_i - F_{i-1}) \tag{2}$$

where $F_i = U_{i,j,k}$. As position and velocity are linked by $U = \mathrm{d}x/\mathrm{d}t$, local transport and position are related by $F = \mathrm{d}r/\mathrm{d}s$, where $s = t/(\Delta x_j \Delta y_j \Delta z_k)$ is a scaled time variable, and $\Delta x_j \Delta y_j \Delta z_k$ is the volume of the grid box. Defining $\beta = F_i - F_{i-1}$ and $\delta = -F_{i-1} + \beta r_{i-1}$, Equation 2 can be written the following way:

$$\frac{\mathrm{d}r}{\mathrm{d}s} - \beta r + \delta = 0 \tag{3}$$

Using the initial condition $r(s_0) = r_0$ the time dependency of r within the considered grid box can be solved analytically and is given by:

$$r(s) = \left(r_0 - \frac{\delta}{\beta}\right) e^{\beta(s-s_0)+\frac{\delta}{\beta}} \tag{4}$$

As these relations only apply inside a given grid cell, the time s_1 when a given particle switches to another cell, that is the time where r is equal to its exit value r_1 must be determined. It is given by the following expression:

$$s_1 = s_0 + \frac{1}{\beta} \log\left[\frac{r_1 - \frac{\delta}{\beta}}{r_0 - \frac{\delta}{\beta}}\right] \tag{5}$$

Using equation 2, the logarithmic factor can also be written as $\log[F(r_1)/F(r_0)]$. A crossing time in the zonal direction can only be obtained if F_i and F_{i-1} have the

same sign, which implies that $F \neq 0$ in the cell. Similar calculations are performed in the two other directions. The shortest difference $\Delta s = s_1 - s_0$ gives the traveling time in the considered cell, and the corresponding face through which the particle escapes. If the particle reaches the zonal face first, its final position on the meridional and vertical axes is then deduced from the previous equations using $s = \Delta s$. Computations are performed for the next cell, with the initial point equal to the final point of the previous cell. The "age" of the particle is then the sum of the obtained Δs.
This method enables both forward and backward integrations to investigate either the fate or the origin of a given water mass.

3.3 Datasets

Water masses generally move along isopycnals. Thus it seems more physical to average at fixed potential density than at fixed depth, in order to capture the correct average transport. We define the mean transports averaged on time at fixed depth and fixed density respectively as $[\mathbf{U}]_z \equiv \overline{\mathbf{U}}$ and $[\mathbf{U}]_\sigma \equiv \widehat{\mathbf{U}}$. In terms of a velocity field $\mathbf{u}_\sigma$[5] and a density layer thickness h_σ, the time-averaged transports can be written:

$$\overline{\mathbf{U}_\sigma} = \overline{\mathbf{u}_\sigma}\,\overline{h_\sigma} \tag{6}$$

$$\widehat{\mathbf{U}_\sigma} = \overline{\mathbf{u}_\sigma h_\sigma} \tag{7}$$

$$\widehat{\mathbf{U}_\sigma} - \overline{\mathbf{U}_\sigma} = \overline{\mathbf{u'}_\sigma h'_\sigma} \tag{8}$$

where $\mathbf{u}_\sigma = \overline{\mathbf{u}_\sigma} + \mathbf{u}'_\sigma$ and $h_\sigma = \overline{h_\sigma} + h'_\sigma$. Equation 8 defines the eddy-induced transport as the correlation between the velocity and the density layer thickness perturbations. There is a difference in the result of a mean whether it has been calculated at fixed depth z or at fixed density σ. If we project $\overline{\mathbf{U}_\sigma}$ back on depth coordinates it will equal $[\mathbf{U}]_z$. The difference $\widehat{\mathbf{U}} - \overline{\mathbf{U}}$ also equals the eddy-induced transport, or bolus transport.
Eddies only appear in high-resolution ocean general circulation models in which the viscosity is not too large. In low-resolution ones, they are usually introduced using a parametrisation. In OCCAM, $\widehat{\mathbf{U}}$ and $\overline{\mathbf{U}}$ are calculated explicitely from the archived data.
The annual mean velocity field and density computed either at fixed depth or at fixed density were used in this study. Consequently the bolus transport is the sum of the real eddies and the seasonal eddies, that is the correlation between the seasonal variations of the velocity field and the isopycnals thickness.

[5]Hereafter, the σ index denotes a variation in x, y, σ and t

4 Results and Discussion

A Lagrangian particle tracking technique has been used to study the origin and fate of the water masses in the Atlantic Ocean as modelled in OCCAM, as these techniques provide us with both the trajectories of the particles, and the associated mass transport.
All calculations have been made with the annual mean dataset, and both with and without the bolus transport contribution in order to estimate the eddy-induced effect in OCCAM results.

4.1 The Conveyor's upper and lower limbs

In order to follow the path of NADW and its return flow in the Atlantic ocean as modelled in OCCAM, Lagrangian particle tracking techniques have been used between the two geographical sections defined as follows:

- a section corresponding to $34°S$ in the Atlantic Ocean;
- a section corresponding to $60°N$ in the Atlantic Ocean.

4.1.1 The Conveyor's upper limb

The calculations for the upper limb were made using elementary particles of 10^{-3} Sv transport at the $34°S$ section, and following them forward up to the $60°N$ section. The only criteria set at the initial section were a potential density σ_0 smaller than 27.6 and particles having a northward velocity. This choice was made because overturning cells at the equator in the Atlantic show that division between NADW outflow and its return flow occurs at this density.
At the final section the following distinction was made according to the density:

- Surface Water ($\sigma_0 \leq 26.5$);
- Subpolar Mode Water ($26.5 < \sigma_0 \leq 27.0$);
- Upper Intermediate Water ($27.0 < \sigma_0 \leq 27.4$);
- Lower Intermediate Water ($27.4 < \sigma_0 \leq 27.6$);
- NADW ($27.6 < \sigma_0$); as it is possible that a part of the flow downwells before reaching $60°N$, this density class can also be interesting.

The quantitative results for the upper limb are presented in Tables 1 and 2. They show relatively important differences depending whether the eddies are taken into account. The bolus transport increases the total mass transport between $34S°$ and $60°N$ by more than 10% (+0.68 Sv). In both cases, the flow begins being exclusively lighter than the critical density $\sigma_0 = 27.6$. At least half of the flow is Surface Water as it crosses $34°S$. When it crosses the final section, hardly any Surface Water can be found, and at least 4 Sv are now Intermediate Water. A part of the flow has even crossed the critical density and been converted to NADW.
However, the total amounts of transport calculated both with eddies and without

(respectively 7.16 and 6.48 Sv) are much below the results from other calculations or observations. Indeed, the admitted transport for the return flow of the Conveyor in the Atlantic Ocean is in the range 13 to 14 Sv [4, 7, 13, 14]. Roughly 50% of the return flow of the Conveyor downwells in the North Atlantic Ocean in the OCCAM model. This is spurious and due to the drift[6] of the model. So at the equator the Conveyor in OCCAM is still in agreement with observations, but further north it becomes too weak.
The paths found for the upper limb both with and without eddies are quite comparable (Figure 1). The flow crosses the $34°S$ section at the Benguela Current and the South Atlantic Ocean by the Southern South Equatorial Current (SSEC). It reaches the strong western boundary current between $15°S$ and $25°S$. The path followed by the Benguela Current and the SSEC is consistent with *Stramma and England, 1999*. They also evidenced a southward shift from $25°S$ to $15°S$ of the northward extent of the subtropical gyre with depth which is not obvious in the calculated path. The flow crosses the equator within the North Brazil Current (NBC). The Equatorial Undercurrent (EUC) is present [16]. The EUC retroflects in the Central South Equatorial Current (CSEC), Eastern South Equatorial Current (ESEC) and Northern South Equatorial Current (NSEC), as found by *Stramma and England, 1999*. A part of the NBC retroflects in the EUC and the Northern Equatorial Counter Current (NECC) as found by *Schott et al., 1998*. Consequently, a part of the northward-flowing water crosses $10°N$ in the basin interior via the NECC and the Northern Equatorial Undercurrent (NEUC), whereas the flow crosses $10°S$ almost exclusively in the western boundary current [2]. The flow then enters the Caribbean Sea and the Gulf of Mexico before flowing out back into the Atlantic. With the bolus calculation about 10 Sv (7 Sv without the eddy-induced effect) flows through the Straits of Florida. About 15 to 30 Sv (the transport depending on the strength of recirculations) follow the American coast to Cape Hatteras as a very narrow flow in the Florida Current. From Cape Hatteras, the flow leaves the coast and flows northwest in the Gulf Stream. A part of the flow participates in the North Atlantic subtropical gyre and is brought back to the Caribbean Sea. The flow finally crosses the $60°N$ section just north of Scotland.
The main eddy-induced differences take place in the strength of the retroflections. The North Atlantic subtropical gyre is enhanced by eddies. So are the retroflections of the NBC and NECC. The general paths between the two section are very similar, except for the SEC whose path is shifted to the south by the eddies.

4.1.2 The Conveyor's lower limb

The calculations for the lower limb were made using elementary particles of 10^{-3} Sv transport at the $34°S$ section, and following them backward up to the $60°N$ section. The only criterion made at the initial section was that the potential density σ_0 had to be greater than 27.6 with a southward velocity. This choice was made because the separation between upper layer waters and deep waters is situated around this

[6]The drift results from the fact that the model has not run during a long enough time to reach a steady state.

density in OCCAM.
The calculated water transports for the lower limb are 7.87 Sv with the bolus calculation and 7.36 Sv without. This flow at $60°N$ is mainly composed of heavy waters (75% with potential density $\sigma_0 < 27.6$). Once again, there is a quite large difference of transport depending whether the eddy-induced effect is taken into account (0.51 Sv), but it is smaller than for the upper limb. This means that most NADW is formed at a more northern latitude than $60°N$, which is consistent with observations. Indeed, most of NADW is thought to form between Iceland and Greenland as the Greenland-Iceland-Scotland Ridge overflow entrains some lighter waters [4]. Once again, the paths of the trajectories obtained by both calculations are very similar (Figure 2). The flow crosses $60°N$ mainly off the coast of Labrador (80% of the flow), the rest comes from the Greenland-Iceland-Scotland Ridge. This path is quite consistent with observations and measurements which show a flow which mainly follows the coast of Labrador [4]. At $50°N$ a part of the flow is taken into a recirculation in the Newfoundland Basin. Just south of Cape Hatteras most branches of the flow merge in the Deep Western Boundary Current. The flow does not enter neither the Gulf of Mexico nor the Caribbean Seas, passes off the coast of Puerto Rico, and then follows the South American coast, until it crosses $34°S$. At about $20°S$ a small part of the flow crosses the ocean to the east, thus crossing $34°S$ near Africa. The path followed by NADW is quite consistent with previous studies. The main differences take place in the size of the Newfoundland recirculation [13], and the lack of a southward flow at the eastern boundary along Africa [16].
The amounts of southward deep transport (7.87 Sv with the eddy-induced effect, 7.36 Sv without) are again much below the values found in previous studies. NADW transport is generally estimated around $13 - 14Sv$ in the Atlantic [13].
However the comparison of the transports for the upper and lower limbs show an excess of 0.77 Sv of southward flowing deep water with the exact bolus calculation (0.97 Sv without) compared with the northward upper layer flow. A reason for this difference could be some water entering the Arctic Ocean through the Bering Strait and flowing out in the Atlantic Ocean. Because of the high density of the missing water, it is more probably due to Antarctic Bottom Water (AABW) flowing northward in the Atlantic Ocean. Indeed, the North Atlantic Ocean is believed to import about 4 Sv of AABW from the South Atlantic [13].

4.2 Sources of the Mediterranean inflow and fate of the outflow

In order to estimate the interactions between the Conveyor Belt and the Mediterranean inflow and outflow as simulated in the OCCAM models, we decided to follow the water particles between three different sections: one corresponding to the Strait of Gibraltar, and the two previously used for NADW, that is $34°S$ and $60°N$ in the Atlantic Ocean.
For both the inflow and the outflow, the Strait of Gibraltar was set as the initial section, and only the initial density criteria and the direction of the integration were changed: forward calculation for the outflow, backward for the inflow. Elementary particles of 10^{-4} Sv transport were used for both calculations.

The repartition of inflowing and outflowing waters in density classes has also been studied, both at the initial and final sections, in order to see which transformations occur. The locations of upwellings and downwellings of a few density classes have also been plotted to study where these transformations take place.

4.2.1 The Mediterranean inflow

The inflowing waters are hereafter defined as follows:

- Warm Water ($\sigma_0 \leq 26.5$);
- Tepid Water ($26.5 < \sigma_0 \leq 27.0$);
- Cold Water ($27.0 < \sigma_0 \leq 27.4$);
- Very Cold Water ($27.4 < \sigma_0$);

This choice of densities was made because the inflowing waters are mainly upper layer waters.
The transports at the initial and final sections are shown in Tables 3 to 6. The locations of the upwelling through the $\sigma_0 = 27.0$ surface of the waters following the northern route and the downwelling through the $\sigma_0 = 26.5$ of the waters following the southern route have also been studied in order to see where the changes in water properties take place.
Depending whether the bolus calculation was used, the results can be very different. According to the results obtained with the eddy-induced effect, 0.20 Sv entering the Mediterranean have crossed the $60°N$ section and 0.84 Sv have crossed $34°S$, whereas the results are 0.69 Sv having crossed $60°N$ and only 0.27 Sv having crossed $34°S$ when calculated without eddies. The northern flow is dominant without the eddy-induced effect whereas the southern one dominates with it.
However, the trajectories of the particles are quite similar with or without the bolus transport, both for the northern and southern routes (Figures 3 and 4). The flow coming from the north is comparable to the northern part of NADW's path. It crosses the $60°N$ section either off the coast of Labrador or just south of Cape Farewell and heads east towards Europe between 45 and $50°N$. It follows more or less the northern and eastern boundaries of the North Atlantic subtropical gyre, before entering the Mediterranean Sea. Most particles stay north of $30°N$, and the flow crosses $40°N$ mainly east of $30°W$. When obtained without the eddy effect, the flow is narrower and slightly more direct.
The flow coming from $34°S$ follows more or less the same path as the Conveyor's upper limb south of $30°N$. Almost all the water entering the Mediterranean is caught in the North Atlantic subtropical gyre.
The total transport of inflowing water is 1.04 Sv with the bolus calculation and 0.96 without. The generally admitted value for the Mediterranean inflow is about 1 Sv [13], which is consistent with the calculated results.
When calculated without the eddy-induced effect, the water at the $60°N$ section is mainly heavy ($\sigma_0 > 27.0$), and it has been totally converted to light water when it

reaches the Strait of Gibraltar. On the other hand, when the eddy-induced effect is taken into account, the water starts mainly as warm light water, and also ends as light water.
The maps of the upwelling through $\sigma_0 = 27.0$ along the northern route are shown in Figure 5. The upwelling with the eddies occurs mainly along North America, whereas without it occurs almost exclusively along $50°N$. The locations of the first and last upwelling differ only slightly: almost all the last upwelling takes place in the Gulf Stream and in the Gulf of Cadiz because of the turbulent overflow of Mediterranean Water and the resulting barotropic instability. The little discrepancies between the map of the first and last upwelling suggest that there are only a few water transformations for these densities along the path. Without the eddies there is a massive upwelling (0.65 Sv) through the surface $\sigma_0 = 27.0$. It is highly reduced by the eddies (0.07 Sv). As these transformations occur deep below the surface, the properties of water are liable to remain more or less the same. As a consequence the massive upwelling taking place without the eddies does not seem very realistic.
The water which follows the southern route begins at $34°S$ as mainly Warm and Tepid Waters, and also ends at the Strait of Gibraltar as light water. There is no massive downwelling, only a slight cooling of the water along its journey.
The locations of the downwelling through $\sigma_0 = 26.5$ along the southern route are shown in Figure 6. They evidence that most of the first downwelling takes place in the subtropical Atlantic Ocean and also in the eastern equatorial region, with much more water conversion in the southern hemisphere. There is also a strong downwelling in the western boundary current below the equator. There are much more locations of downwelling with the eddy-induced effect than without, but the general areas remain more or less the same. Eddies significantly enhance the downwelling in the Benguela Current, the Florida Current and some parts of the Gulf Stream. A relatively strong downwelling also occurs in the Gulf of Cadiz because of the turbulent entrainment resulting from the overflow. The eddies enhance subduction from the mixed layer to the thermocline after cooling. By this process the transformation from Warm to Tepid Water is enhanced by the eddies.
The effect of eddies on the locations of water transformations is consistent with their effect on the volume of water being transformed: they limit the number of water transformations as well as the volume of water concerned by transformations below the mixed layer by reducing the mass flux divergence and the diapycnal mixing, but they enhance subduction from the mixed layer to the layers below.

4.2.2 The Mediterranean outflow

As the Mediterranean waters are saltier than those in the Atlantic Ocean they are also denser. As a consequence the density classes that were used for the inflow are no longer adapted for this study. The outflowing waters are hereafter defined as follows:

- Upper Intermediate Water ($\sigma_0 \leq 27.0$);

- Middle Intermediate Water ($27.0 < \sigma_0 \leq 27.4$);
- Lower Intermediate Water ($27.4 < \sigma_0 \leq 27.6$);
- Deep Water (DW) ($27.6 < \sigma_0$);

The transports of the outflow for each density class at the initial and final sections are given in Tables 7 to 10. As expected they evidence that the water at the initial section is mainly heavy water: at least 85% of the flow is Deep Water at the initial section [11]. Contrary to the inflow, the southern route (0.57 Sv with eddies, 0.61 without) dominates the northern one both with (0.42 Sv) and without (0.31 Sv) the eddy-induced effect. The proportion of waters from each density class at each section is also similar with and without the bolus calculation. The values at the final section show that the water following the northern route has become lighter whereas the one following the southern route has become denser.
The paths of the outflowing waters are very similar when calculated with or without the eddy-induced effect (Figures 7 and 8). The main flow of the northern route follows the continental shelf off the coasts of Europe and crosses the $60°N$ section just north-west of Scotland. The rest of it crosses the Atlantic and flows northeastward in the Gulf Stream before crossing the final section just west of Scotland.
The flow following the southern route crosses the Atlantic to the west between 30° and $40°N$ before going southward in the DWBC, thereafter following a route very similar to NADW outflow. Considering the density of the outflowing water when is crosses the $34°S$ section ($\sigma_0 > 27.6$), it means that this water has mixed with NADW. It then seems consistent that it follows the same path.
The total amount of water outflowing the Mediterranean Sea is 0.99 Sv with the bolus transport and 0.92 Sv without. These values are very similar to the total transport of inflowing water. As the Strait of Gibraltar is the only way to leave the Mediterranean Sea (the transport through the Suez Channel is neglectable), the inflowing and outflowing transports should be exactly the same. The difference between the two values is 0.05 Sv which is probably due to rounding errors in the given transports. These results are consistent with the 1 Sv estimated transport of the Mediterranean outflow [13].
It is possible to study where the downwelling of outflowing Intermediate Water occur along the northern route. The corresponding maps are shown in Figure 9. First, a very important transformation of water takes place just at the overflow at the Strait of Gibraltar and in the Gulf of Cadiz. There is a significant downwelling of Intermediate Water at this location due to the intense mixing taking place. The maps of the last location of the upwelling of DW show that most of it takes place in the western Atlantic Ocean, and especially in the Florida Current and just west of Scotland and Ireland. The Deep Water that upwells along the west coast of America goes to the north whereas the Deep Water that does not upwell flows to the south.

5 Conclusion

We have investigated the thermohaline circulation in the Atlantic Ocean and the role of the Mediterranean Sea in this circulation as modelled in OCCAM. A Lagrangian method which enables to trace a water mass as a set of elementary trajectories was used. This technique consists in successive integrations of a stationary three-dimensional velocity field over the model grid. A considerable amount of particles is needed for a global picture of the flows. Two datasets were employed in order to investigate the eddy-induced effect in OCCAM. One of them only uses annual mean velocities, the other includes the eddy-induced transport velocity.
Different water masses were tracked in the Atlantic Ocean: the return flow of the Conveyor Belt, the North Atlantic Deep Water, the water which enters and the one which leaves the Mediterranean Sea. A quantitative estimation of the total mass transport and of the transformations along the path as well as a qualitative picture of the main pathways of the flow were performed for each water mass.
The total transport for both NADW and its return flow evidenced too many water transformations in the North Atlantic Ocean in OCCAM because of the drift of the model. Consequently the calculated transports north of the equator are about twice as weak as the estimations resulting from observations. South of the equator the transports are in agreement with observations. However, the pathways of the flows seem generally consistent with previous studies and observations. Eddies seem to have a small effect on NADW and its return flow in the Atlantic. They mainly enhance recirculations and increase the total transport.
The quantitative results for the Mediterranean inflow and outflow are more in agreement with expected values. They evidence the existence of two origins for the inflowing waters: one from the north (Labrador Sea) and one from the south (Benguela Current). These two contributions are unequal: without eddies the southern route dominates the northern one, with the eddies the southern part recedes. When eddies are accounted for, inflowing waters start mainly as light waters. The outflow is also divided between north and south. A smaller part contributes to the NADW return flow going to the north, the largest part is entrained within NADW at the western boundary and flows to the south after crossing the Atlantic. The eddies have a significant effect on water transformations: they limit the water conversions below the mixed layer, but enhance the subduction from the mixed layer to the layers below.
The qualitative results evidence the major role played by the subtropical gyres and the western boundary current system. The eddies generally enhance recirculations.
These results will be used in an inter-comparison study of the Conveyor Belt by the TRACMASS project team. In particular, the results of the Mediterranean inflow and outflow will be compared with that of a similar study carried out by the Italian TRACMASS team using the French OPA model.
We also calculated the sources of the Atlantic Equatorial Undercurrent with the same methodology. The results of that study will be reported elsewhere.

Appendix

The OCCAM model

The primitive equations

The state of the ocean can be defined by the temperature, salinity and three components of velocity. The temperature is usually replaced by the potential temperature because it remains constant under adiabatic changes in pressure. Oceans are actually rather described by temperature (or potential temperature), three components of velocity and density (or potential density), because salinity is defined by an international standard which represents the combined effects of the different dissolved salts in the ocean.
The evolution of the ocean can be specified using a momentum equation to give the time change in velocity, and an advection-diffusion equation for the changes in temperature and salinity. The system also needs a continuity equation, an equation of state and boundary conditions.
In order to reduce the computational load, the three following approximations are often made in ocean models:

- the ocean is incompressible;
- the vertical velocity is small and the terms involving it in the vertical momentum equation are neglectable;
- small changes in density can be neglected in the horizontal momentum equation, except where they affect the horizontal pressure gradient.

The equations resulting from these approximations were called the 'primitive equations' by Bryan. The horizontal momentum equation is:

$$\frac{\partial \mathbf{u}}{\partial t} + (\mathbf{u} \cdot \nabla)\mathbf{u} + w\frac{\partial \mathbf{u}}{\partial z} + f \times \mathbf{u} = -\frac{1}{\rho_0}\nabla p + \mathbf{D_u} + \mathbf{F_u} \tag{9}$$

The three dimensional advection/diffusion equations are,

$$\frac{\partial S}{\partial t} + (\mathbf{u} \cdot \nabla)S + w\frac{\partial S}{\partial z} = \mathbf{D}_S + \mathbf{F}_{S'} \tag{10}$$

$$\frac{\partial T}{\partial t} + (\mathbf{u} \cdot \nabla)T + w\frac{\partial T}{\partial z} = \mathbf{D}_T + \mathbf{F}_{T'} \tag{11}$$

and the pressure (or vertical momentum), incompressibility and density equations are,

$$\rho g = -\frac{\partial p}{\partial z} \tag{12}$$

$$\nabla \cdot \mathbf{u} + \frac{\partial w}{\partial z} = 0 \tag{13}$$

$$\rho = \rho(T, S, p) \tag{14}$$

The prognostic variables are $\mathbf{u}$ the horizontal velocity, T the potential temperature, and S the salinity. The other variables, p the pressure, w the vertical velocity and

ρ the density, can be calculated from the prognostic ones from equations 12, 13 and 14 respectively.
In these equations t is time, f is the Coriolis term ($f = 2\Omega \sin\Theta$), where Ω is the Earth's rotation rate and Θ the latitude. The terms $\mathbf{D}$ represent the diffusion and $\mathbf{F}$ the forcing.
The velocity on all solid boundaries and the gradients of potential temperature and salinity normal to solid boundaries are set to zero. The stress acting on the ocean surface due to the wind and the fluxes of heat and fresh water through the air-sea interface also needs to be specified. An additional friction force at the bottom of the ocean has also been implemented. It is assumed to act horizontally and is given by:

$$\mathbf{F_b} = -0.001\mathbf{u} \mid \mathbf{u} \mid \tag{15}$$

To solve these equations, the ocean is split into a large number of boxes along lines of constant latitude, longitude and depth. Each box is either full of sea water of or solid land, depending on the topography. A box which is full of sea water is called tracer box, tracers being for example potential temperature and salinity. The average values of tracers within each box are specified at its centre.
The velocity field is defined using a second grid, similar to the tracer grid. In the case of the OCCAM model, this second grid is shifted because OCCAM uses an Arakawa-B grid. In such grids, the velocity points are defined at the corners of the tracer grid boxes. Arakawa-B grids are generally preferred in models because they are more accurate than other schemes.

OCCAM grids

The numerical model equations are obtained by integrating the primitive equations over each grid box to give an equation where the advective and diffusive terms are replaced by the fluxes through the boundaries of the box, and the other terms are written in terms of average over the box. The discrete timestep has to be large enough to be computationally efficient, but small enough to be numerically stable. Because of the convergence of meridians at the poles, models using regular latitude-longitude grids require smaller timesteps in polar regions to the detriment of computational costs. To overcome the singularity at the North Pole, OCCAM is split into two different models, Model 1 and Model 2.
Model 1 uses a regular latitude-longitude grid which covers the Pacific and Indian Oceans from $78.25°S$ to $66°N$, and the South Atlantic Ocean from $78.25°S$ to $0°$, with a resolution of $0.25°$ both in latitude and longitude. This corresponds to a resolution of about 25 km at the equator.
Model 2 uses a rotated latitude-longitude grid and covers the North Atlantic and Arctic Oceans with a resolution of $0.25°$ both in latitude and longitude. The grid is rotated so that it matches the Model 1 grid at the equator. The North pole of the Model 2 grid is at the intersection of the Equator and $118°W$, and the South Pole on the Equator and $62°E$.
The two models are connected through the Bering Strait by a simple channel model.

The model has 36 levels in the vertical, which thickness varies from 20 m at the surface to 255 m at a depth of 5500 m.

References

[1] Blanke, B., and S. Raynaud, Kinematics of the Pacific Equatorial Undercurrent: an Eulerian and Lagrangian approach from GCM results, *J. Phys. Oceanogr., 27*, 1038-1053, 1997.

[2] Blanke, B., M. Arhan, G. Madec and S. Roche, Warm water paths in the Equatorial Atlantic as diagnosed with a general circulation model, *J. Phys. Oceanogr., 29*, 2753-2768, 1999.

[3] Broecker, W. S., The great ocean conveyor, *Oceanography, 4*, 79-89, 1991.

[4] Dickson, R. R., and J. Brown, The production of North Atlantic Deep Water: Sources, rates, and pathways, *J. Geophys. Res., 99*, 12,319-12,341, 1994.

[5] Döös, K., Interocean exchange of water masses in the Southern Ocean, *J. Geophys. Res., 100*, 13,499-13,514, 1995.

[6] Drijfhout, S. S., E. Maier-Reimer, and U. Mikolajewicz, Tracing th conveyor belt in the Hamburg large-scale geostrophic ocean general circulation model, *J. Geophys. Res., 101*, 22,563-22,575, 1996.

[7] Gordon, A. L., Interocean exchange of thermocline water, *J. Geophys. Res., 91*, 5037-5046, 1986.

[8] Holland, W. R., and P. B. Rhines, An example of eddy-induced ocean circulation, *J. Phys. Oceanogr., 10*, 1010-1031, 1980.

[9] Holland, W. R., T. Keffer, and P. B. Rhines, Dynamics of the oceanic general circulation: the potential vorticity field, *Nature, 308*, 698-705, 1984.

[10] Lozier, M. S., Evidence for large-scale eddy-driven gyres in the North Atlantic, *Science, 277*, 361-364, 1997.

[11] Price, J. F., and M. O'Neil Baringer, Outflows and deep water production by marginal seas, *Prog. Oceanog., 33*, 161-200, 1994.

[12] Reid, J. L., On the contribution of the Mediterrannean Sea outflow to the Norwegian-Greenland Sea, *Deep-Sea Res., 26A*, 1199-1223, 1979.

[13] Schmitz, W. J., Jr., and M. S. McCartney, On the North Atlantic circulation, *Rev. Geophys., 31*, 29-49, 1993.

[14] Schmitz, W. J., Jr., On the interbasin-scale thermohaline circulation, *Rev. Geophys., 33*, 151-173, 1995.

[15] Schott, F. A., J. Fischer, and L. Stramma, Transports and pathways of the upper-layer circulation in the Western Tropical Atlantic, *J. Phys. Oceanogr., 28*. 1904-1928, 1998.

[16] Stramma, L., and M. England, On the water masses and mean circulation of the South Atlantic Ocean, *J. Geophys. Res., 104*, 20,863-20,883, 1999.

Table 1: Origin and fate of the upper limb with eddies

	$34°S$	$60°N$
Surface	4.29	0.02
Subpolar	1.70	1.76
Upper Int.	0.94	4.13
Lower Int.	0.23	0.44
NADW	0.00	0.81
Total	7.16	7.16

Table 2: Origin and fate of the upper limb without eddies

	$34°S$	$60°N$
Surface	3.07	0.00
Subpolar	1.92	1.35
Upper Int.	1.30	3.79
Lower Int.	0.19	0.92
NADW	0.00	0.42
Total	6.48	6.48

Table 3: Origin and fate of the northern inflow with eddies

	$60°N$	Gibraltar
Warm	0.13	0.14
Tepid	0.00	0.06
Cold	0.01	0.00
Very cold	0.06	0.00
Total	0.20	0.20

Table 4: Origin and fate of the northern inflow without eddies

	$60°N$	Gibraltar
Warm	0.00	0.29
Tepid	0.04	0.40
Cold	0.27	0.00
Very cold	0.38	0.00
Total	0.69	0.69

Table 5: Origin and fate of the southern inflow with eddies

	$34°S$	Gibraltar
Warm	0.47	0.22
Tepid	0.28	0.47
Cold	0.07	0.15
Very cold	0.02	0.00
Total	0.84	0.84

Table 6: Origin and fate of the southern inflow without eddies

	$34°S$	Gibraltar
Warm	0.12	0.03
Tepid	0.11	0.23
Cold	0.03	0.01
Very cold	0.01	0.00
Total	0.27	0.27

Table 7: Origin and fate of the northern outflow with eddies

	Gibraltar	$60°N$
Upper Int.	0.03	0.04
Middle Int.	0.03	0.23
Lower Int.	0.01	0.11
Deep	0.35	0.04
Total	0.42	0.42

Table 8: Origin and fate of the northern outflow without eddies

	Gibraltar	$60°N$
Upper Int.	0.02	0.03
Middle Int.	0.03	0.20
Lower Int.	0.01	0.06
Deep	0.25	0.02
Total	0.31	0.31

Table 9: Origin and fate of the southern outflow with eddies

	Gibraltar	$34°N$
Upper Int.	0.03	0.00
Middle Int.	0.04	0.00
Lower Int.	0.02	0.00
Deep	0.48	0.57
Total	0.57	0.57

Table 10: Origin and fate of the southern outflow without eddies

	Gibraltar	$34°N$
Upper Int.	0.03	0.00
Middle Int.	0.05	0.00
Lower Int.	0.01	0.00
Deep	0.52	0.61
Total	0.61	0.61

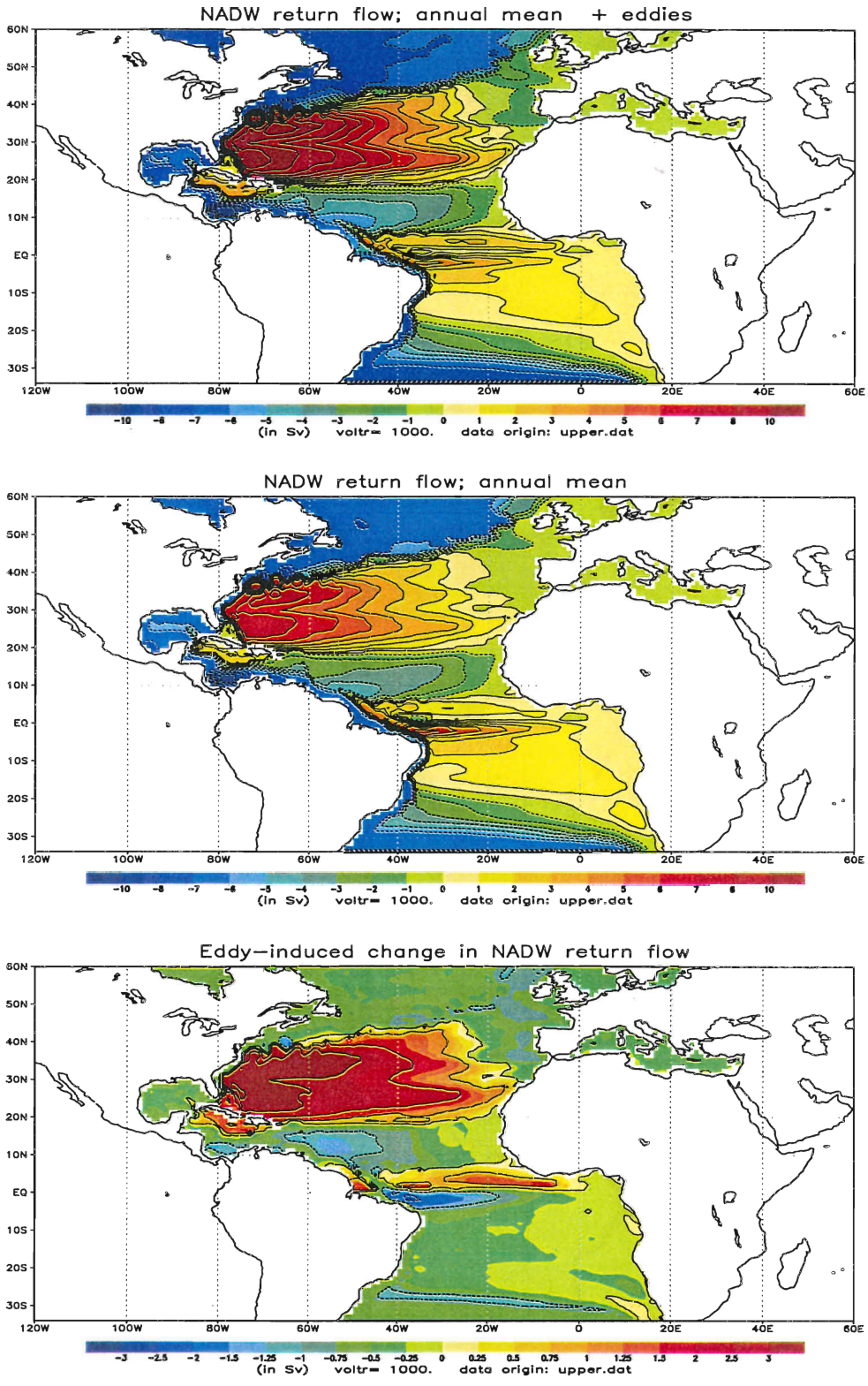

Figure 1: Paths of the return flow of the Conveyor in the Atlantic

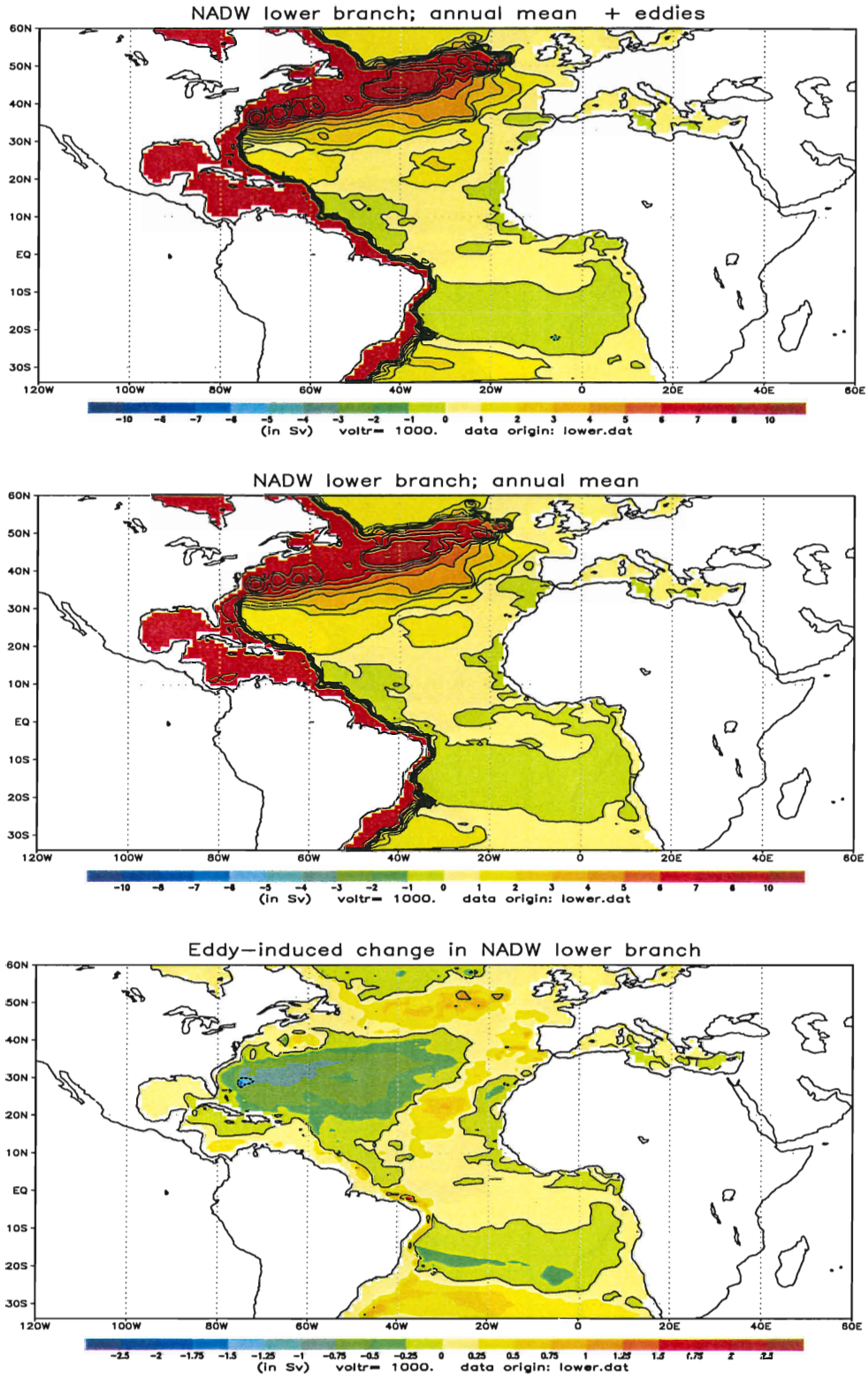

Figure 2: Paths of NADW lower limb in the Atlantic

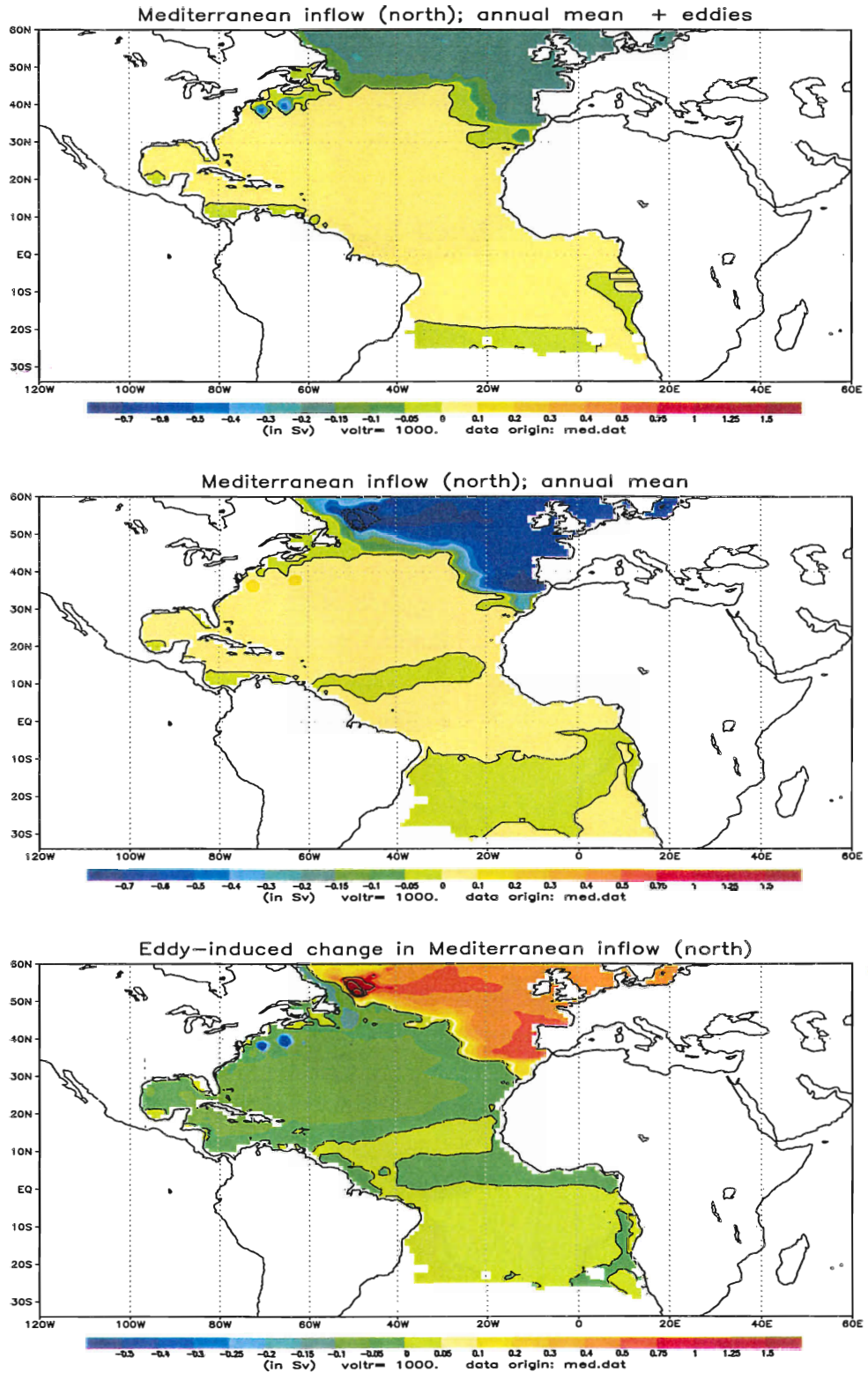

Figure 3: Paths of the northern route of the Mediterranean inflow

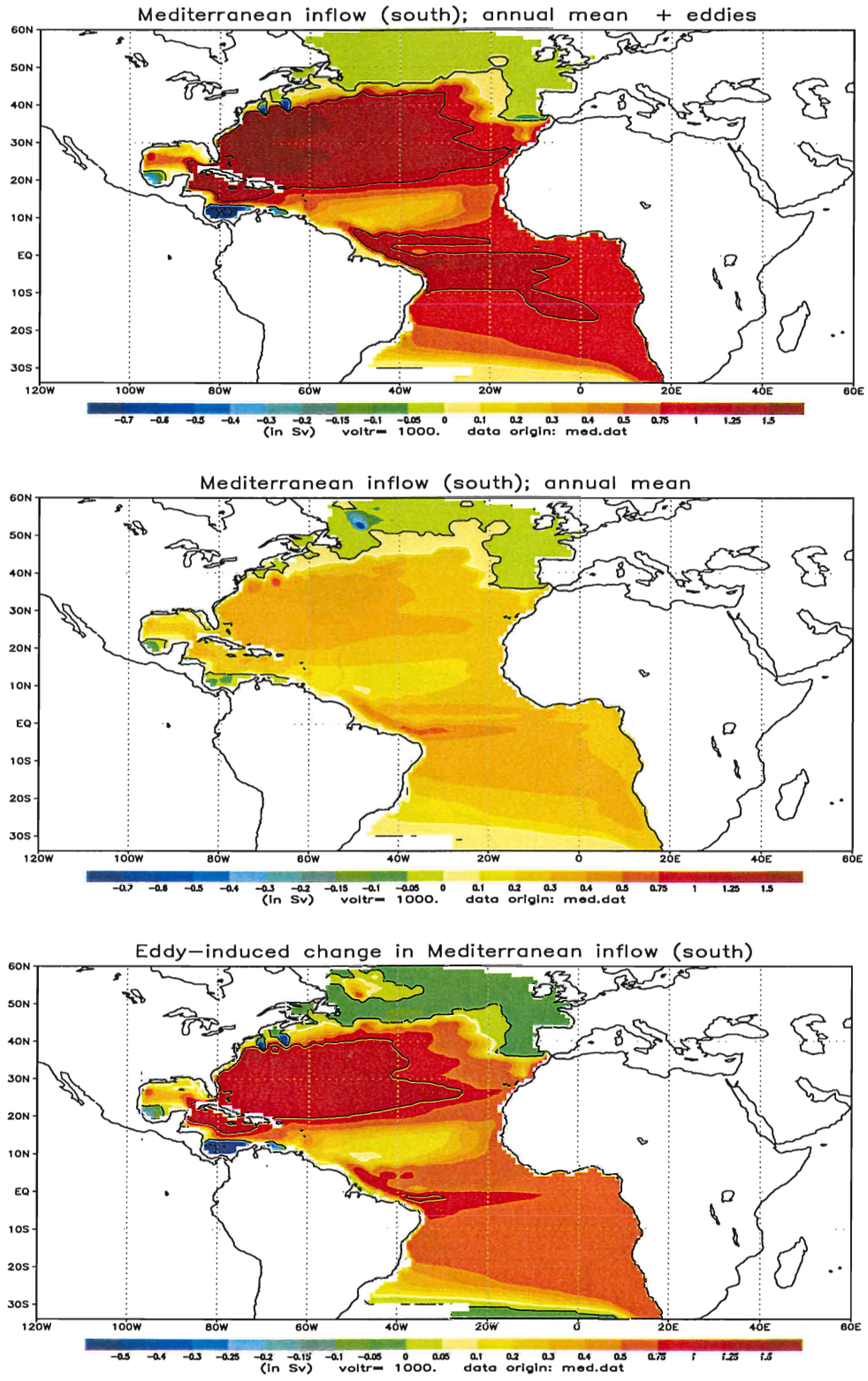

Figure 4: Paths of the southern route of the Mediterranean inflow

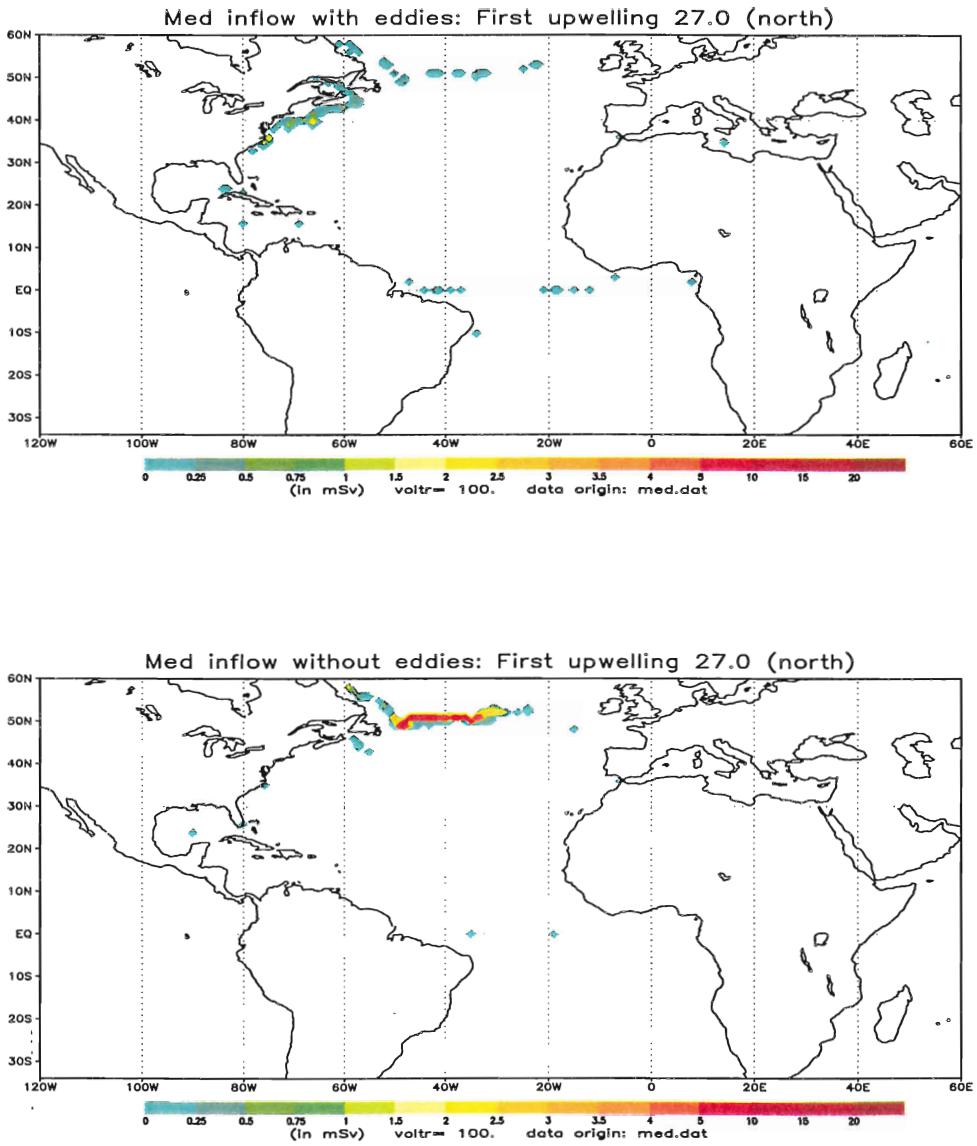

Figure 5: Locations of the upwelling through $\sigma_0 = 27.0$ for the inflowing northern route

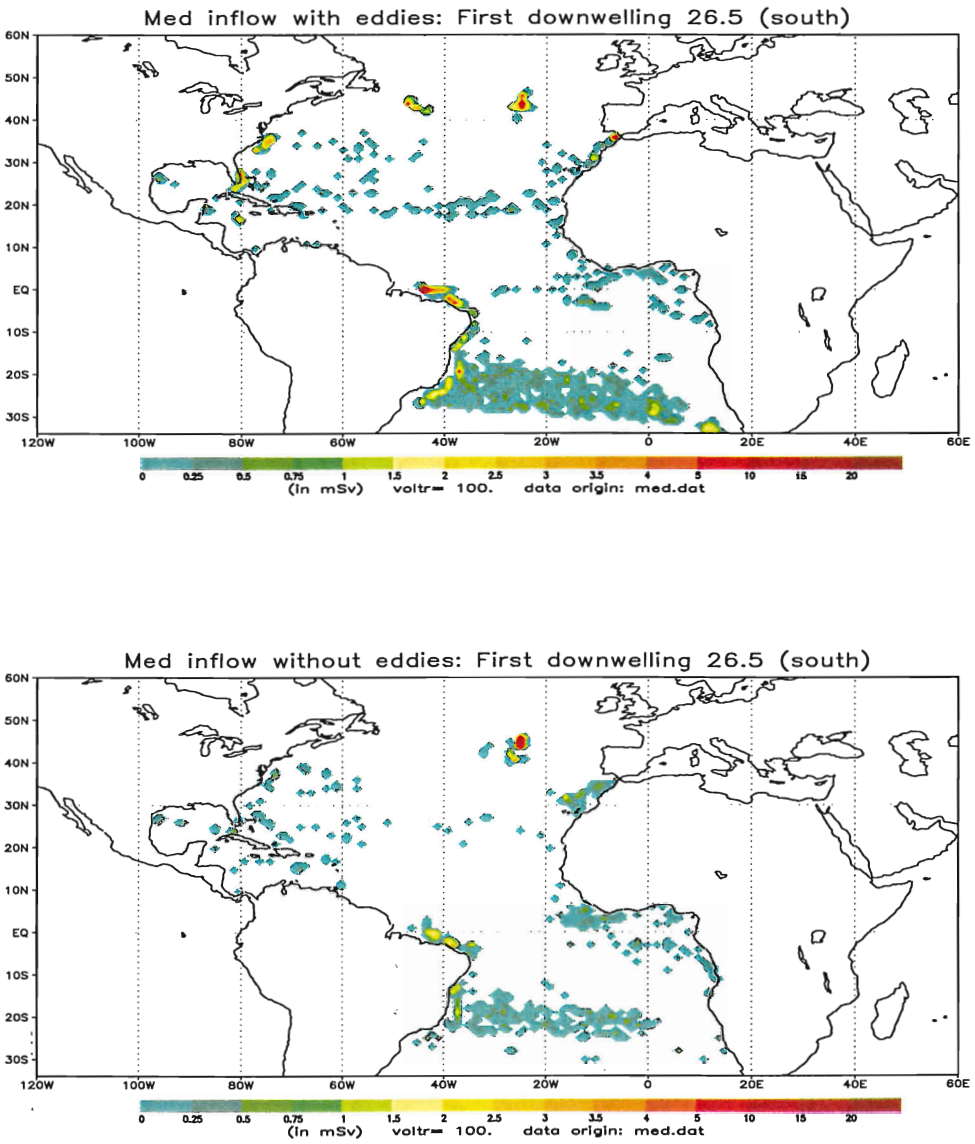

Figure 6: Locations of the downwelling through $\sigma_0 = 26.5$ for the inflowing southern route

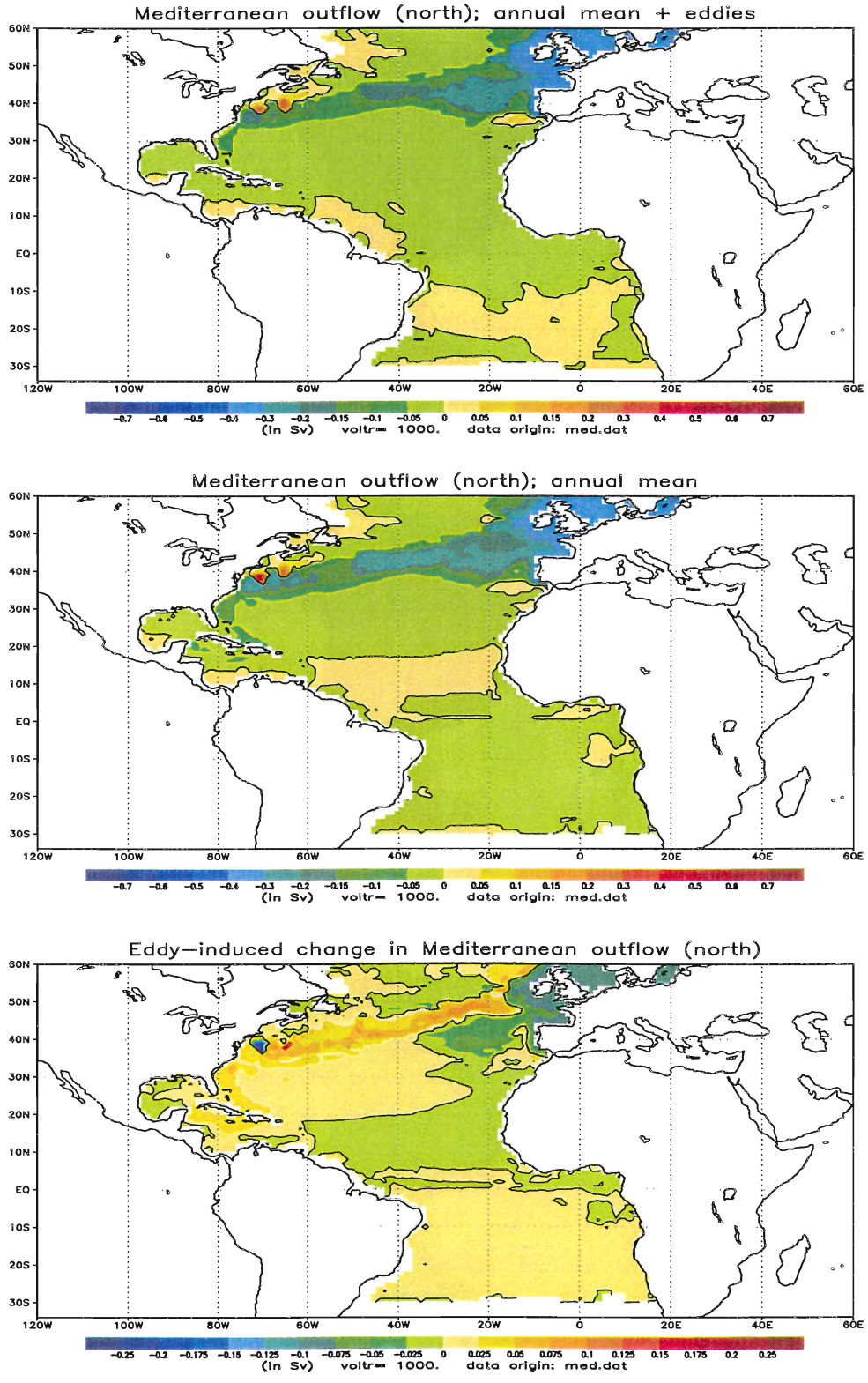

Figure 7: Paths of the northern route of the Mediterranean outflow

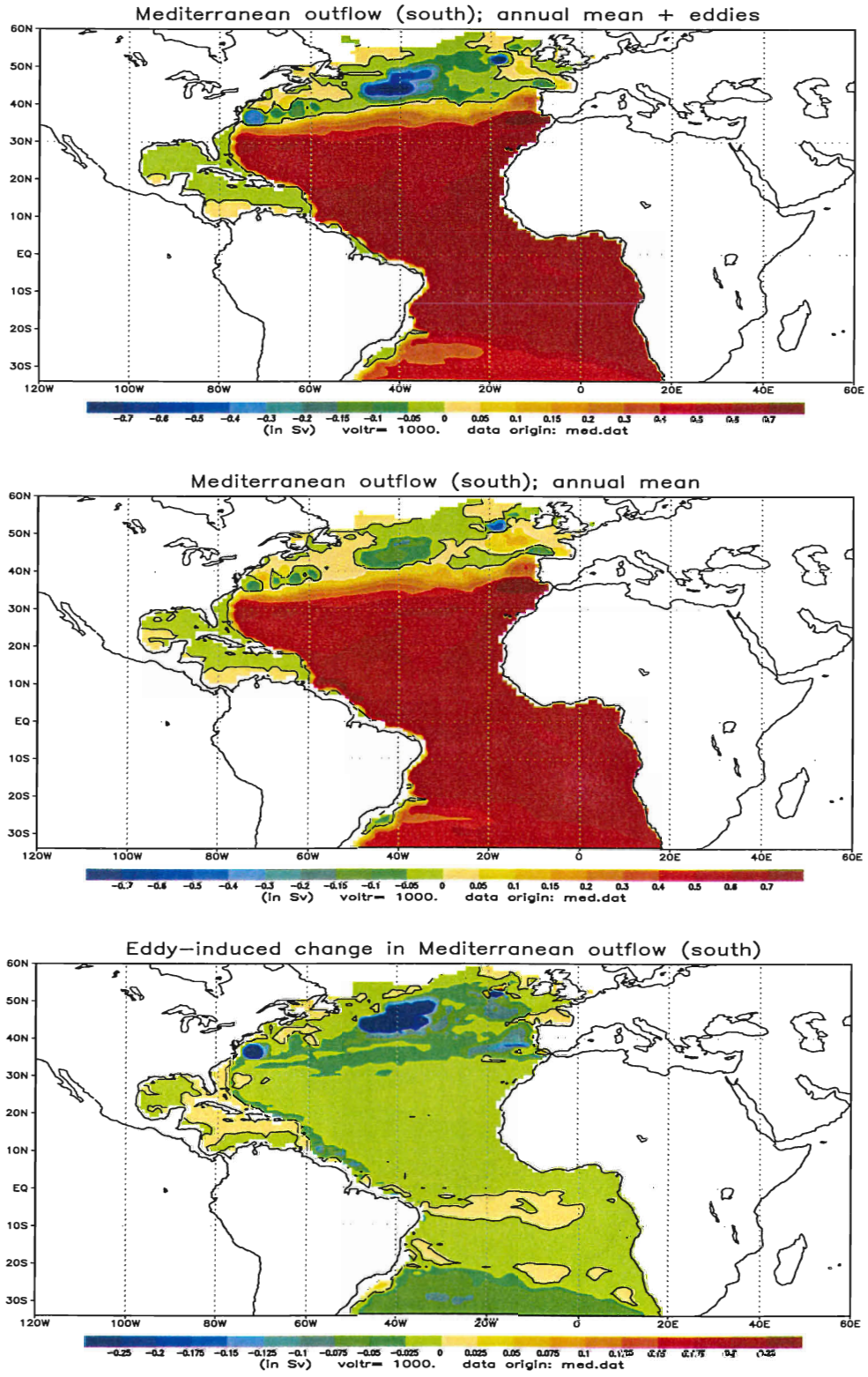

Figure 8: Paths of the southern route of the Mediterranean outflow

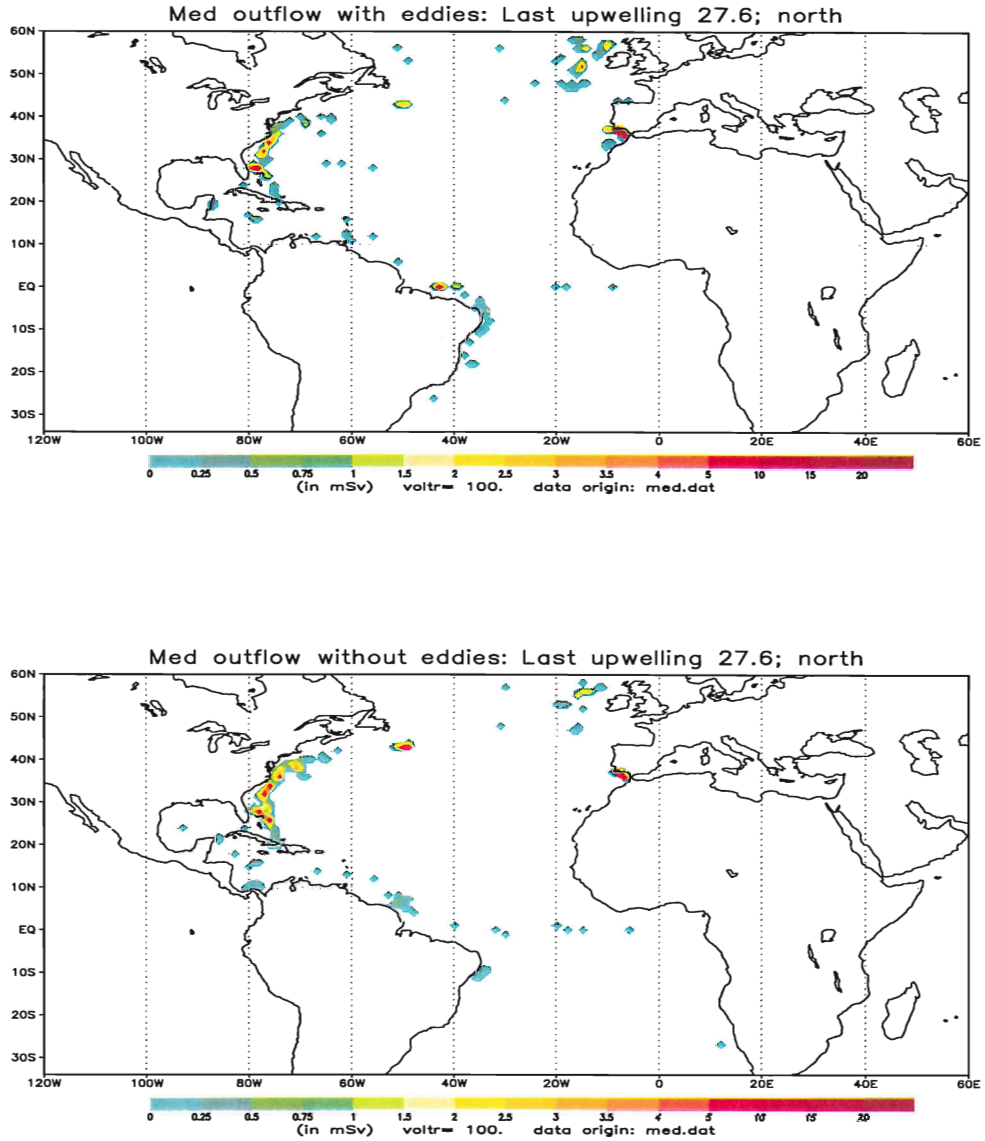

Figure 9: Locations of the upwelling through $\sigma_0 = 27.6$ for the outflowing northern route

OVERZICHT VAN KNMI-PUBLICATIES, VERSCHENEN SEDERT 2000

KNMI-PUBLICATIE MET NUMMER

186-II Rainfall generator for the Rhine Basin: multi-site generation of weather variables by nearest-neighbour resampling / T. Brandsma a.o.

186-III Rainfall generator for the Rhine Basin: nearest-neighbour resampling of daily circulation indices and conditional generation of weather variables / Jules J. Beersma and T. Adri Buishand

186-IV Rainfall generator for the Rhine Basin: multi-site generation of weather variables for the entire drainage area / Rafal Wójcik, Jules J. Beersma and T. Adri Buishand

188 SODA workshop on chemical data assimilation: proceedings; 9-10 December 1998, KNMI, De Bilt, The Netherlands

189 Aardbevingen in Noord-Nederland in 1998: met overzichten over de periode 1986-1998 / [Afdeling SO]

190 Seismisch netwerk Noord-Nederland / [afdeling Seismologie]

191 Het KNMI-programma HISKLIM (HIStorisch KLIMaat) / T. Brandsma, F. Koek, H. Wallbrink, G. Können

192 Gang van zaken 1940-48 rond de 20.000 zoekgeraakte scheepsjournalen / Hendrik Wallbrink en Frits Koek

193 Science requirements document for OMI-EOS / contr. by R. van der A .. [et al.] **(limited distribution)**

194-1 De zonsverduistering van 11 augustus 1999, deel 1: de waarnemingen van het gedrag van flora en fauna / J. Kuiper, m.m.v. Guus Kauffeld

195 An optimal infrasound array at Apatity (Russian Federation) / Läslo Evers and Hein Haak **(limited distribution)**

196-I Rainfall Generator for the Meuse Basin: simulation of 6-hourly rainfall and temperature for the Ourthe catchment / Rafal Wójcik and T. Adri Buishand

TECHNISCH RAPPORT = TECHNICAL REPORT (TR)

219 De invloed van de grondwaterstand, wind, temperatuur en dauwpunt op de vorming van stralingsmist: een kwantitatieve benadering / Jan Terpstra

220 Back-up modellering van windmeetmasten op luchthavens / Ilja Smits

221 PV-mixing around the tropopause in an extratropical cyclone / M. Sigmond

222 NPK-TIG oefendag 16 december 1998 / G.T. Geertsema, H. van Dorp e.a.

223 Golfhoogteverwachtingen voor de Zuidelijke Noordzee: een korte vergelijking van het ECMWF-golfmodel (EPS en operationeel), de nautische gidsverwachting, Nedwam en meteoroloog / D.H.P. Vogelezang, C.J. Kok

224 HDFg library and some hdf utilities: an extention to the NCSA HDF library user's manual &reference guide / Han The

225 The Deelen Infrasound Array: on the detection and identification of infrasound / L.G. Evers and H.W. Haak

226 2D Variational Ambiguity Removal / J.C.W. de Vries and A.C.M. Stoffelen

227 Seismo-akoestische analyse van de explosies bij *S.E. Fireworks* ; Enschede 13 mei 2000 / L.G. Evers e.a.

228 Evaluation of modified soil parameterization in the ECMWF landsurface scheme / R.J.M. IJpelaar

229 Evaluation of humidity and temperature measurements of Vaisala's HMP243 plus PT100 with two reference psychrometers / E.M.J. Meijer

230 KNMI contribution to the European project WRINCLE: downscaling relationships for precipitation for several European sites / B.-R. Beckmann and T.A. Buishand

231 The Conveyor Belt in the OCCAM model: tracing water masses by a Lagrangian methodology / Trémeur Balbous and Sybren Drijfhout

232 Analysis of the Rijkoort-Weibull model / Ilja Smits

233 Vectorization of the ECBilt model / X. Wang and R.J. Haarsma

234 Evaluation of a plant physiological canopy conductance model in the ECMWF land surface scheme / J. van de Kassteele

235 Uncertainty in pyranometer and pyrheliometer measurements at KNMI in De Bilt / J.S. Henzing and W.H. Knap

236 Recalibration of GOME spectra for the purpose of ozone profile retrieval / Ronald van der A

237 Tracing water masses in the Atlantic / Yann Friocourt and Siebren Drijfhout

WETENSCHAPPELIJK RAPPORT = SCIENTIFIC REPORT (WR)

00-01 A model of wind transformation over water-land surfaces / V.N. Kudryavtsev et al.

00-02 On the air-sea coupling in the WAM wave model / D.F.Doortmont and V.K. Makin.

00-03 Salmon's Hamiltonian approach to balanced flow applied to a one-layer isentropic model of the atmosphere / W.T.M. Verkley

00-04 On the behaviour of a few popular verification scores in yes-no forecasting / C.J. Kok

01-01 Hail detection using single-polarization radar / Iwan Holleman

01-02 Comparison of modeled ozone distributions with ozonesonde observations in the tropics / Rob Put

01-03 Impact assessment of a doppler wind lidar in space on atmospheric analyses and numerical weather prediction / G.J. Marseille, A. Stoffelen, F. Bouttier, C. Cardinali, S. de Haan and D. Vasiljevic.

KNMI-bibliotheek, postbus 201, 3730 AE De Bilt, tel. 030 - 2 206 855, fax 030 - 2 210 407; bibliotheek@knmi.nl